Mahammad Abdul HANNAN[1], Farid Arafat AZIDIN[2], Azah MOHAMED[1]

Universiti Kebangsaan Malaysia (1), Universiti Teknikal Malaysia Melaka (2)

Light Vehicle Energy Management System using Multi-Power Sources

Abstract. This paper describes the modelling of the energy management system (EMS) of light vehicles using hybrid multi-power source systems. The hybrid system included a fuel cell (FC), a battery, supercapacitors (SC) and a photovoltaic cell. The battery was used as the primary power source for driving the vehicle. Other sources were used as supplemental power sources for medium range vehicle usage. The control algorithm was developed as a switching mechanism used to trigger between the energy sources based on the drive of the vehicle power system as a means of examining the electrical power flow. The control algorithm was used to manage the switching operation of power supplies for the EMS during light vehicle operation. The results showed that the models were operating efficiently based on the switching control algorithm and management of the energies from various sources.

*Streszczenie. Opisano modelowaniem system zarządzania energią lekkich pojazdów. W skład systemu wchodzą: bateria, superkondensator i bateria fotowoltaiczna. Szczególną uwagę zwrócono na mechanizm przełączania między źródłami energii. (**System zarządzania energią w lekkich pojazdach mechanicznych**)*

Keywords: Fuel cell, PV, supercapacitors, energy management system.
Słowa kluczowe: lekkie pojazdy mechaniczne, bateria, zarządzanie energią.

Introduction

Light vehicles, such scooters or auto rickshaws, are important modes of transportation in many Asian countries, including Malaysia and Indonesia [1, 2]. The energy source of these vehicles comes from fossil fuels that have a negative impact on the cities through pollution and noise. Multi-power sources from renewable energies can be implemented as an alternative fuel source in electric light vehicles. The renewable energies that can be used practically in vehicles include FC, solar, battery and SC. These four energy sources may be used in concert so that vehicles may have sufficient power and energy capacity in the future.

This paper focuses on the energy management system (EMS) to coordinate the four energy sources so that the vehicle can consume less energy and produce higher power capacity. The system can select which sources drive the electrical motor depending on vehicle driving conditions and the capacity of the sources. As a matter a fact, all renewable energy sources have weaknesses in either power or energy density [3, 4, 5]. For instance, FCs have high energy density but low power density and a start time that takes several seconds or even a minute to get into full operation. By creating an effective coordination system, the different energy sources can be used to assist each other, making the system compatible for light vehicle usage. Another important design consideration for the EMS is to use a maximum amount of energy from the solar energy harvester and a minimum amount of energy from the fuel cell.

In the motor drive system, energy is normally supplied from a single source, such as a power grid [6, 7]. A control system is only required to drive the motor. A basic open loop motor drive system is shown in Fig. 1 [8, 9, 10].
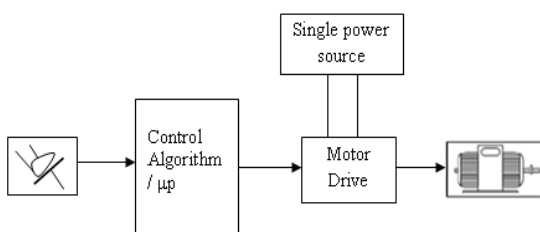

Fig. 1. A basic open loop motor drive system

In the case of multi-power sources, an EMS is needed to manage the power system before the load. The block diagram for multi-power sources in an open loop system is shown in Fig. 2 [11].
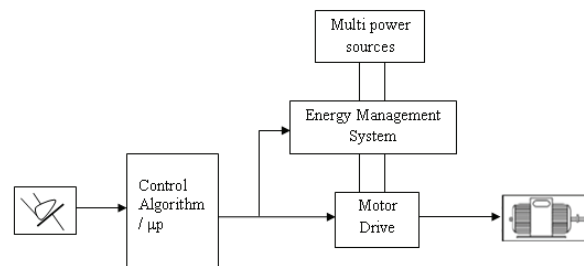

Fig. 2. An open loop motor drive system with multi-power sources

The concept of a motor drive system for multi-power sources is shown in Fig. 3 [9]. The block diagram inside the dashed line is the EMS. For single-source motor drive systems, the microprocessor has only a single task: to produce a PWM signal to drive the electric motor. Additionally, a power regulator may be required to maintain the power supply. In a multi-power system, an EMS with a control algorithm is required to coordinate the power sources for consistent supply. In this case, the microprocessor has two tasks: to drive the motor and to control the multi-power sources. As mention earlier, the following PSPICE simulation only models the electrical system design and electrical flow according to a control algorithm.

In the EMS design, the control algorithm will only control three sources, the FC, battery and SC, while solar energy will directly charge the battery. As a result, it is necessary that the battery has storage capacity for energy harvesting through solar panels or when it is plugged into the grid. Unlike other hybrid electric vehicle designs, which use a combustion engine or fuel cell as the primary source [5,12, 13, 14, 15, 16], this system uses the battery as the primary energy source. The FC is used as an extended source, and the SC is used under high power conditions. All three sources require a dc-dc boost converter to drive the motor at the rated voltage.
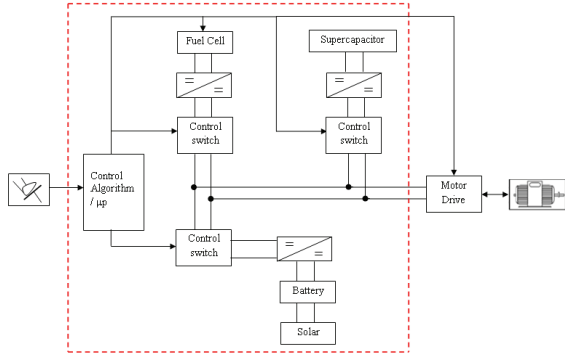
Fig. 3. A multi-power source motor drive system

Modelling Framework
Theoretical Model
The theoretical model contains the three multi sources and boost/buck converters. First, a literature review of the three sources is discussed, and the PSPICE simulation is then described.

FC Model
An FC is an electrochemical device that produces DC electrical energy through a chemical reaction. It consists of an anode, anode catalyst layer, electrolyte, cathode and cathode catalyst layer. A multiple fuel cell will be arranged either in series or parallel in a stack to produce the desired voltage and current. The type of FC that is suitable for vehicle operation is a proton exchange membrane fuel cell (PEMFC). The PEMFC is solid polymer FC that uses a special plastic membrane as an electrolyte. The primary fuel in PEMFC is hydrogen [17, 18].

The overall chemical reaction between hydrogen and oxygen is described in the formulae below [19]:

$$(1) \qquad H_2 + \frac{1}{2} O_2 \longrightarrow H_2O$$
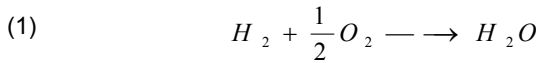
where ΔG is the change in Gibbs free energy formation. The byproducts of the chemical reaction are heat and water/steam. The overall reaction proposed in an acidic medium is

$$(2) \qquad O_2 + 4H^+ + 4e^- \longrightarrow 2H_2O$$
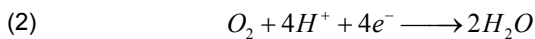
The theoretical voltage, E, is produced under fuel cell standard conditions of 25°C and 1 atmosphere of pressure. Electrical work is described as work done by charge, Q, when moving in electric field across a voltage, E. Thus, the relationship can be expressed as

$$(3) \qquad \Delta G = Q E$$
$$(4) \qquad Q = n F$$

The relationship between these two equations is

$$(5) \qquad \Delta G = n F E$$

where n is constant parameter for equation (4) and (5).The theoretical voltage, E, generated by the FC varies depending on the partial pressures of hydrogen and oxygen, systems pressure and operating temperature. The following empirical model describes the current/voltage relationship for the PEMFC [20]:

$$(6) \qquad V = E - ir - A \ln\left(\frac{i + i_n}{i_o}\right) + m\, e^{(ni)}$$

The constant of r, m and n are empirical parameters that function of the operations. The term V is voltage produce of fuel cell and E is generated voltage of a single cell. Because the FC energy source can be simulated like other energy sources, even though it has a slow transient response), an FC model is designed as a combination of a voltage source and an RC circuit. The voltage source is fixed according to the voltage value of the FC, and the RC circuit is a delay time to adjust for the slow dynamics of the FC. The time delay of the output response of the FC can be calculated as [8]

$$(7) \qquad T = 2\pi \sqrt{R C}$$

The start-up time of the FC depends on manufacturer specifications and can be range from seconds to minutes. Because the PSPICE software is a limited edition, only a few seconds of time delay could be simulated. The output voltage of the FC for the simulation is listed in Table 1.

Battery Model
In the EMS, the battery can be charged during regenerative braking and from residual energy of the FC under a low or no load power system. In this stage, the battery acts as an energy storage device. At the same time, the battery can supply energy continuously to the load. The disadvantage of the battery is it has a limited number of lifetime cycles.

Internal resistance in the battery shows inconsistent performance during charge and discharge. It behaves linearly during discharge but subsequently drops 25% of its state of charge (SoC) due to increases in internal resistance. The battery SoC can be defined as [11, 12]:

$$(8) \qquad SoC(t) = \frac{1}{Q_{bat}} \int_{t_0}^{t} i_{bat}(t) \cdot dt + SoC_0(t_0)$$

The capacity of a lead-acid battery can be calculated using Peukert's equation (11). The equation implies that at higher current, there is less available energy in the battery. The theoretical capacity of the battery, C, is described in terms of current, I; the total charge time, T; and the Peukert number, k, which lies between 1.2 and 1.4 for acid batteries [4].

$$(9) \qquad C = I^k T$$

Another lead-acid battery model is described for lead acid batteries. The model determines the SoC according to the current drawn from the battery. The remaining of SoC can be related to the capacity of the battery in Ampere-hour, C_1, which is expressed as a percentage. The equation of SoC in terms of discharge time, T_s, and current, I_{bat}, is defined as [4].

$$(10) \qquad SoC = 1 - \frac{I_{bat} T_s}{C_1 \, 3600}$$

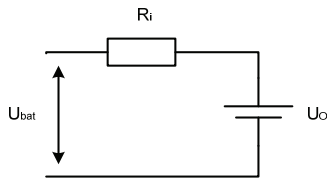A simple battery model can be described by using the equivalent circuit shown in Fig. 4.

Fig.4. Simple battery equivalent circuit

SC Model

An SC is an electrochemical capacitor that offers high power density compared to other storage devices. It contains an electrical double layer and separator that separates and holds electrical charges. Consequently, the separation of charges provides a small energy potential, as low as 2 to 3 V [21]. The double layer is made of a nanoporous material, such as activated carbon, that can improve storage density. Supercapacitors capacity can be as high as 3000 farads. Using the basic capacitor model for the SC, voltage $V_C(t)$ can be expressed in the following equation (2), where $i_c(t)$ is the charging capacitor current and $V_o(t_0)$ is initial voltage of capacitor [12]:

$$(11) \qquad V_c(t) = \frac{1}{C} \int_{t_0}^{t} i_c(t) \cdot dt + V_o(t_0)$$

SC (800-1500F) can be modeled as high-power but low capacity batteries. It stores electrical energy by accumulating and separating opposite charges. Batteries, however, store energy chemically in reversible chemical reactions. One advantage of SC is that it has excellent lifecycles. The lifecycle of SC can be in the range of 105 – 106, and they are expected to last as long as a car [22]. It efficiency is 90%, as compared to batteries [4]. SC has low energy density, in the range of 5-10 Wh/kg, while batteries have an energy density range of 30-40 Wh/kg [21].
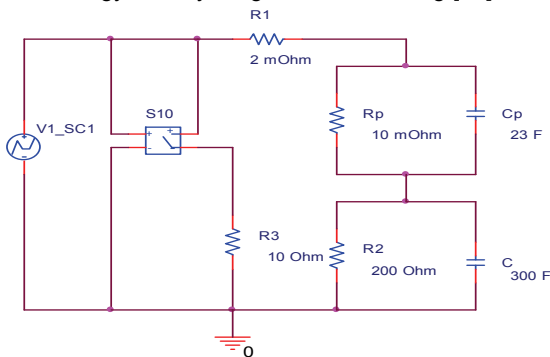

Fig. 5. A PSPICE model of a SC

The model of SC used in the measurements was the SPICE model ECOND Pscap350 SC [22]. The SPICE model was built using experimental charging and discharging results from a SC and then plotting the data to yield the voltage response over time. Using these experimentally measured results, a model was developed. The simulation model schematic is shown in Fig. 5. Changes were made by replacing the current source with a voltage source to fit our simulation purposes. During execution, the SC voltage was fixed at 5.4 V. The equations for the parameter values are as follows:

$$(12) \qquad C = \frac{\Delta Q}{\Delta U}$$

$$(13) \qquad C_p = \frac{C}{C_1}$$

$$(14) \qquad R_1 = \frac{\Delta U}{\Delta i}$$

where parameters ΔQ, ΔU, Δu and Δi refer to the plotted graph of screening test using ECOND Pscap350 [23].

$$(15) \qquad R_3 = \frac{\Delta t}{-\ln\left(\frac{U_1}{U_o}\right) C}$$

DC/DC buck Converter for FC Model

The FC output voltage is 60 V and rated motor voltage is 48 V. A step down DC voltage is required to convert the FC to the rated voltage. The basic DC/DC buck converter circuit is shown in Figure 6. The input voltage is controlled by a switch, and the control switch is triggered by the period of the duty cycle, D_C, defined as [24]:

$$(16) \qquad D_C = \frac{t_{ON}}{T}$$

where T is a constant period and ton is the length of the ON state of the switch. The function of diode D2 is to ensure the return path for the inductor current when the switch is open. The LC filter circuit provides continuous output voltage that equals the average output value of the rectangular waveform. From the constant input voltage, V_{in}, the average output voltage, V_o, can be defined by

$$(17) \qquad V_0(t) = \frac{1}{T} \int_0^{t_{ON}} V_i(t) \cdot dt = D_C \cdot V_i$$

Assuming no power losses and a dc/dc converter efficiency of $\eta = 1$, the duty cycle can be calculated as:

$$(18) \qquad P_i = P_o$$

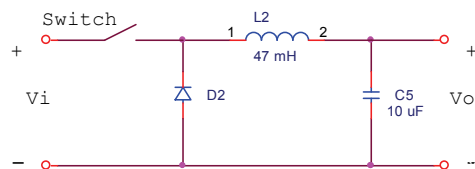$$(19) \qquad \frac{V_o}{V_i} = \frac{I_i}{I_o} = D_C$$

Fig. 6. A PSPICE model of a dc/dc buck converter

In the PSPICE simulation in Figure 4, the switch in Figure 6 is replaced by switch module S2, and the control signal was replaced by pulse module VPULSE.

DC/DC boost Converter for FC Model

The SC circuit is linked to the dc/dc boost converter to raise voltage from 2x2.7 V to 48 V dc motor voltages. The step-up converter is shown in Figure 7. When the diode is reverse biased, the inductor stores energy from the input voltage [24] according to the equation,

$$(20) \qquad V_i = L \frac{di_L}{dt}$$

where i_L is the inductor current. Thus, the energy transfer from input voltage source, V_i, to output voltage source, V_o, can be described as

$$(21) \qquad V_i - V_o = L \frac{di_L}{dt}$$

The following ON and OFF switch time period conditions were applied,

(22)
$$\frac{V_i}{L} t_{ON} = \frac{V_i - V_o}{L} t_{off}$$

The input and output voltage as a function of the duty cycle, DC, can be expressed as,

(23)
$$\frac{V_o}{V_i} = \frac{T}{t_{off}} = \frac{1}{1 - D_C}$$

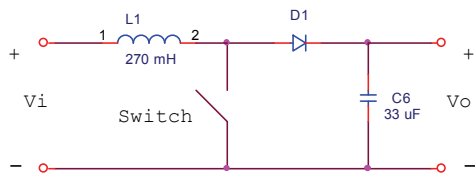A schematic diagram is shown in Fig. 7.

Fig. 7. A PSPICE model of the dc/dc boost converter

Simulation Model

The simulation model in the PSPICE circuit design contained three basic circuits, including the EMS, photovoltaic source and shunt regulator, and basic dc motor drive circuit designs.

EMS Circuit Design

The PSPICE model for the EMS is for a dc motor rated power of 5 kW. It is based on the reference model of an FC powered scooter with a rated power of 3.6 kW and an auto rickshaw in India with rated power of 6 kW [1]-[2], [19]. The capacity of the energy sources is shown in Table 1.

Table 1. Specification of multi-power sources

Component/Parameter	Specifications
PEMFC	5kW, 60V, 83.5A
Battery	5kW(Lithium), 48V, 100Ah
Solar	200 W, V_{mp} 43.6 V, I_{mp} 4.6 A
Supercapacitor/Ultracapacitor	2x2.7V, 1200 F

The battery is used as the primary energy source for the electric vehicle. Thus, it is important that the energy required by the dc motor can be supplied by the battery without any assistance from the other sources. The specification of a 48 V battery was chosen because it is the same rated voltage as the motor electric vehicle. The energy density from the battery should allow the vehicle to travel in short distance. For extended distances, the fuel cell is used and recharges the battery simultaneously. The PEMFC is used because it is more compatible as a vehicle power source and uses hydrogen as a fuel source. The power rating of 5 kW was selected because it can provide both power and energy to the vehicle. Solar power can be harvested during the day, and a reasonable area on the vehicle that can be used to collect solar energy is between 1-1.5 m2. Technically, the power that can be produced is around 200-240 W given the efficiency of current generation solar collectors. The maximum voltage and current values are taken from the Trunsun Solar datasheet. The SC comes from Maxwell technologies and is rated at 2.7 V for each SC; in this simulation, however, a 5.4 V SC is used.

The PSPICE model of the multi-power sources in the EMS is shown in Fig. 8. The three power source models are the SC v1_sc1, fuel cell v2_fc1 and battery v4_batt. A dc booster converter is required to raise the voltage of the SC from 5.4 V to 48 V, and a dc buck converter is used to step down the rated voltage of the fuel cell from 60 V to 48 V. The controller is three switches, S6, S7 and S8, which are operated based on the algorithm of the EMS. The three sources are then linked to simple dc motor drive that consists of two switches, S11 and S12, and two flywheel diodes for regeneration braking before being connected to the load. The load is assembled using a pure resistive 1 kΩ load.
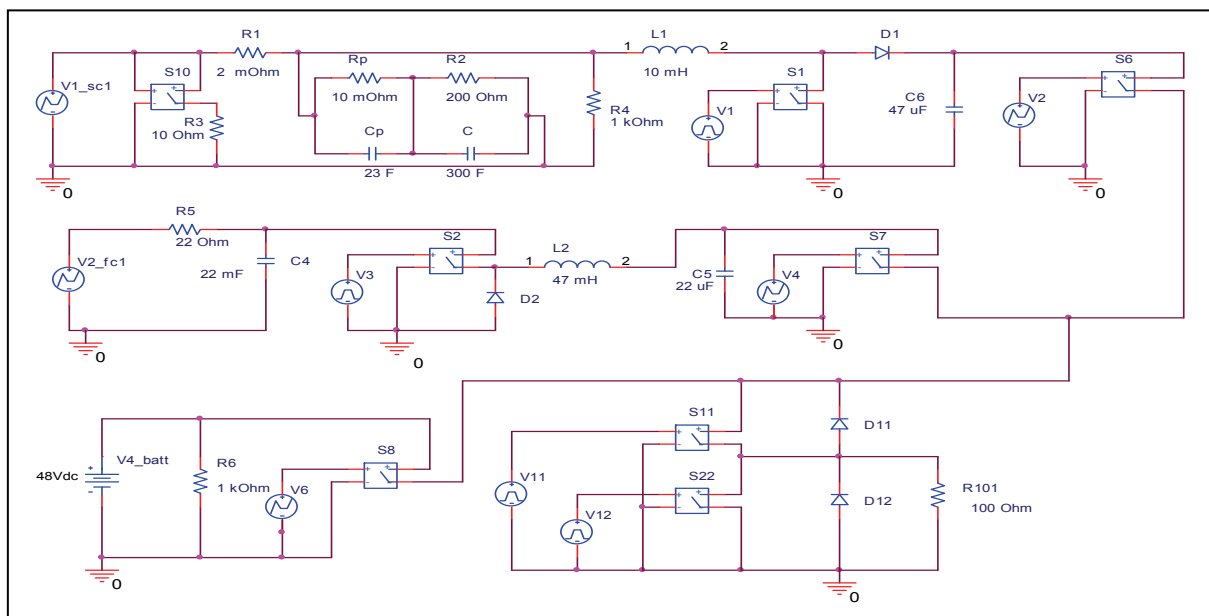

Fig.8. A PSPICE model of multi-power sources connected to the load

Photovoltaic Source and Shunt Regulator Circuit Design

The idea of using solar energy to supplement the operation of a small vehicle is technically feasible because of its modest power requirements. An example of a suitable solar-powered vehicle is the two-wheeled vehicle that is widely used in many Asian countries [1]-[2], [25]. The power consumption for this vehicle is around 3-6 kW, and a 250 W solar module can contribute about 5-8% of the operational needs of the vehicle. If the vehicle is not extensively used, the percentage is increased. Besides solar energy being a renewable resource, solar-powered vehicles also reduce pollution in the city. This would have a substantial impact in many Asian countries where these kinds of vehicles are extensively manufactured each year [1]-[2].

The daily average solar radiation is inconsistent [22, 26, 27]. As a result, solar modules are usually designed to charge the battery first before it can be used as a consistent supply source. Because of this reason, a photovoltaic source is not directly controlled by the EMS. Fig. 9 shows the photovoltaic source circuit that is combined with a shunt regulator. Table 1 shows that the output voltage is set by a voltage source, V2, and connected to a boost converter to yield 48 V output voltages. It is then linked to a shunt regulator to avoid battery overcharge.
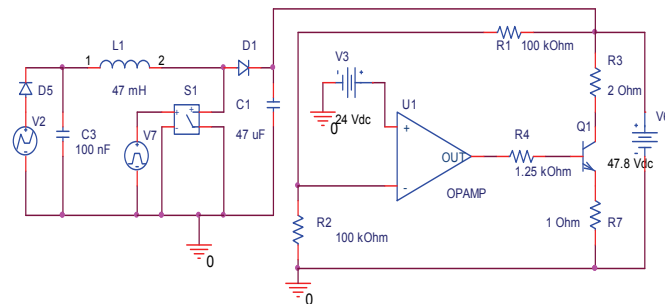

Fig.9. A PSPICE model of a photovoltaic source link to a shunt regulator

Basic dc Motor Drive Circuit

The PSPICE model of the drive motor and load are derived from the step-down chopper [8], [23]. The switch, S11, and diode, D12, control the motor speed and torque, respectively. The switch, S22, and diode, D11, allow the motor to act as a generator when regenerative braking occurs. A resistive load is implemented that has a value of $R_{101} = 100\Omega$.
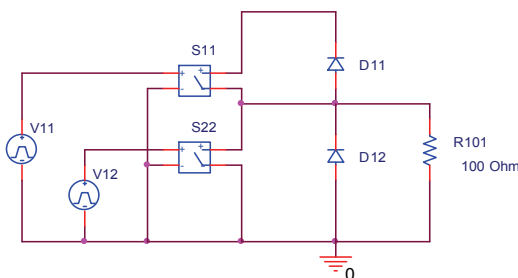

Fig. 10. A basic dc motor drive circuit

EMS Control Algorithm

All of the energy sources have different tasks in delivering power to the load. The EMS controls the energy sources and their tasks are defined as follows:
i.   The battery is the main energy source of the vehicle. When the start button is triggered, processors will determine the battery capacity and pedal acceleration. The energy management system will then decide which

energy sources should activate according to the control algorithm strategy. The battery also functions as a storage device and receives charge from the fuel cell and solar panel.
ii. The FC is the secondary energy source of the vehicle. It will start by supplying energy to the load and, at the same time, recharging the battery when the battery capacity falls below 40%. If the battery reaches 80% of its capacity, then the FC supply is cut off unless high power demand is required. Any excess energy from the FC will be stored to the battery. By using this new concept of proportion energy, the use of hydrogen in the FC can be reduced.
ii. The SC is a supporting energy source when both the battery and fuel cell take a long time to support high power condition. After it has triggered, it will recharge and wait for the next coming request.
iv. Solar energy is considered as an additional source of energy. The main task is to harvest energy during the day and directly recharge the battery.

Operational Control Strategy

The three energy sources are controlled by three switches: S6, S7 and S8 (see Fig. 8). A control algorithm is designed to fulfill the condition based on driving conditions and to maximize energy conservation [28, 29, 30, 31]. The control algorithm descriptions in logic are explained in the following table [32, 33].

The operational control strategies are based on six operation states. The main task of the system is to maintain the power source to drive dc motor. The control system should be intelligent enough to recognize situations and trigger the appropriate state from the aforementioned table. In this work, the controller determines three basic operational input conditions, which include load through pedal offset (PO), power duration load (PD) through measuring motor speed over a long period of time, and battery capacity (BC). In this strategy, the battery plays important role as the primary power source, and the battery capacity is critical in changing the state. The seven operational states are discussed as follows:

Table 2. Control Algorithm in Logic

State	SC S6	FC S7	Battery S8	Condition
1	0	0	0	Off operation/Safety features
2	0	0	1	BC is High; PD is Low and PO is Low
3	0	1	0	BC is Low; PD is Low and PO is Low
4	0	1	1	BC is High; PD is High and PO is Low
-	1	0	0	-- (Not possible)
5	1	0	1	BC is High; PD is Low and PO is High
6	1	1	0	BC is Low; PD is Low and PO is High
7	1	1	1	BC is High; PD is High and PO is High

State 1: (Input: Safety Button; Output: S6 + S7 + S8); off operation. (Safety features)

State 2: (Input: BC + PD + PO; Output: S6 + S7 + S8); Battery will be fully used to drive the motor with no high power demand situation. As a part of conservation energy, the FC stays not in operation and will only become active when the battery capacity is low.

State 3: (Input: BC + PD + PO; Output: S6 + S7 + S8); FC takes over to drive the vehicle and charge the battery until it turns to State 2.

State 4: (Input: BC + PD + PO; Output: S6 + S7 + S8); Consequence of high power demand has forced the system to activate FC as an auxiliary energy source.

State 5: (Input: BC + PD + PO; Output: S6 + S7 + S8); In this state, the battery powered vehicle accelerates with support from the SC. Return to State 2 after all energy in SC is flush out.

State 6: (Input: BC + PD + PO; Output: S6 + S7 + S8); Battery is critical. The FC powered vehicle accelerates with additional energy from the SC. After the SC tank is empty, the system will change to State 3.

State 7: (Input: BC + PD + PO; Output: S6 + S7 + S8); When the vehicle is operated at high speeds and requires acceleration, the system is forced to activate all energy sources.

In this system, the FC operates in ON/OFF operation, which means the opening valve cannot be controlled. This also means that energy from the FC is supplied to the load when it is in full operation. To coordinate the supply load, switches are designed for every energy source. In this case, the three switches S6, S7 and S8 are the output switches controlled by EMS so the current can flow to the load efficiently. The system attempts to manage the operation of the energy sources based on the operational control strategy. Any excess energy will charge the battery, and the motor drive system is designed to implement regenerative braking.

Energy Flow Process

A sample of the energy flow process following the control algorithm strategy is shown in flowchart Fig. 11.
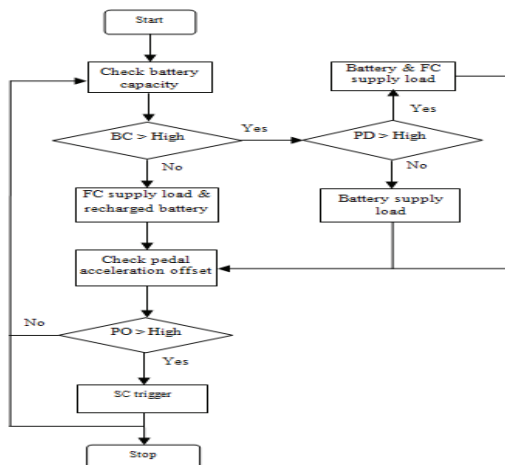

Fig.11. Energy flow process flowchart

The systems rely on three operational inputs, which are not simulated in this simulation because the system uses an open loop system. Overall, the system starts by checking the battery capacity, as the battery is the primary energy source. If there is enough energy stored, the vehicle will be powered by battery or else the FC will be activated and will charge the battery at the same time. Then, the motor speed is checked. If the system detects that the vehicle runs at high speed for a long time, either a combination of battery and FC or only battery is activated. The next process detects the pedal offset to determine sudden power requirements. If the pedal offset is high, then it triggers the SC and rechecks the battery condition.

Results and Discussion

The simulation result looks at the dimension of the component design and switching technique of the energy sources. The load is a pure resistive load as it gives a better graphical result than a RL load. The simulation results start by observation of the FC and SC before and after passing the dc/dc converter and before supplying the load. Fig. 12 shows an output voltages diagram of the sources before and after the dc/dc converter. In this analysis, SC is triggered at 3.5 s and can supply current for at least 2 s. Meanwhile, FC is configured to have a delay time (start-time) of at least 3 s before it can reach the maximum voltage value. The output voltage of FC and SC are rated to 48V from 60 V and 5.4V, respectively. The switching frequency of the buck converter is $f_r = 10$ kHz, with a duty cycle of D = 0.8. The boost converter frequency is $f_r = 2$ kHz with D = 0.9.
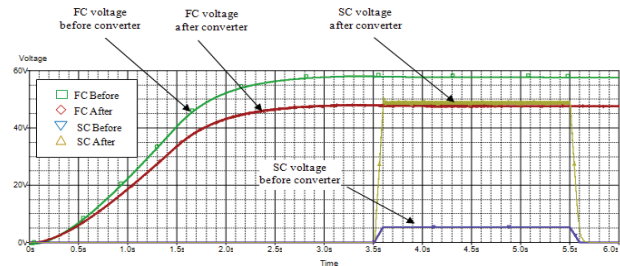

Fig.12. Output voltages before and after the FC and SC

Simulation results in the following graphs are presented according to the state. It is important that the system maintain the voltage supply at the load. Fig. 13 shows when the system operates in State 3, which is when the FC is activated. In this experiment, the FC takes 3 seconds to reach a maximum output voltage; it also takes 3 seconds from maximum to zero voltage after being shut down. A switch, S7, controls the output of the FC and only allows supply to the load when it reaches a maximum output. During the delay time, the excess energy can be used to charge the SC or battery. For this test example, the FC operates for 4 seconds and then cuts off from the system. The objective of this test is to conduct switching and determine the optimal time to allow only a rated voltage to supply to the load. Only the energy under the rated voltage can drive the motor, and energy below rating can be conserved. In that way, the efficiency of the FC can be optimized; this process also helps to overcome the problem of start-time. In the design of the hardware, a delay relay can be implemented, and the time setting can be set according the FC start-time. The problem remains that the design circuit current used to charge the battery during the delay time using freewheeled diode.
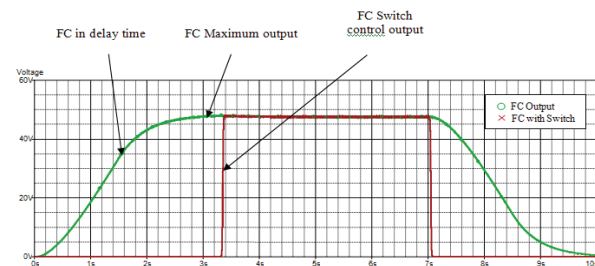

Fig. 13. Output systems when the FC is active

The next example, shown in Fig. 14, is when the vehicle detects that the battery capacity is low and starts to activate the FC. For the first 3 seconds, the battery still supplies a voltage and waits for the FC to reach a maximum output. At this stage, the system is in State 2. After 3 s, the vehicle requires high power energy and forces the system to activate both the battery and FC. As the system no longer requires extensive power, it will turn off the battery and uses

the FC to supply power and simultaneously recharge the battery. This is referred to as State 3 from the correspond figure. At 7 s, the battery has reached sufficient energy capacity and allows the system to activate Stage 2 again. Basically, the system attempts to use the battery as a major supply source. It will activate the FC when the battery energy capacity is low, but the FC has a start-time operation during which the battery must be used to supply power until the FC reaches its maximum operation. If extensive power is required, both the FC and battery must support the system until the power request is reduced, unless the battery is absolutely critical. The different states can be expressed in terms of power:

At the state 2: $P_{load} = P_{battery}$
At the state 3: $P_{load} = P_{FC}$ (where battery is low)
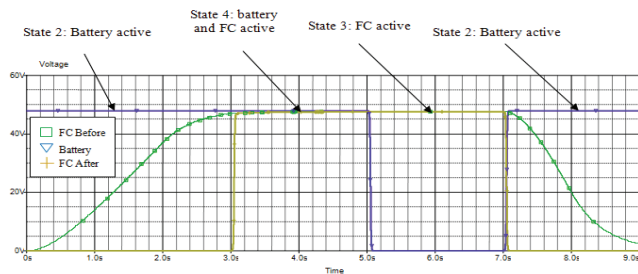At the state 4: $P_{load} = P_{battery} + P_{FC}$

Fig. 14. Output systems at States 2, 3, and 4

In some occasions, such as overtaking or climbing steep hill, the SC will be activated to support the battery during vehicle acceleration. This situation is presented in Fig. 15. The system uses the battery for normal operation or when the control algorithm is in State 2. After 1 s, an auxiliary energy is required and requests the SC to trigger. The energy delivered by the SC allows the vehicle to accelerate until all of the energy exhausted, and it will then automatically shut down. The graph below shows SC support energy from 1 to 3 s. This power system can be defined as,

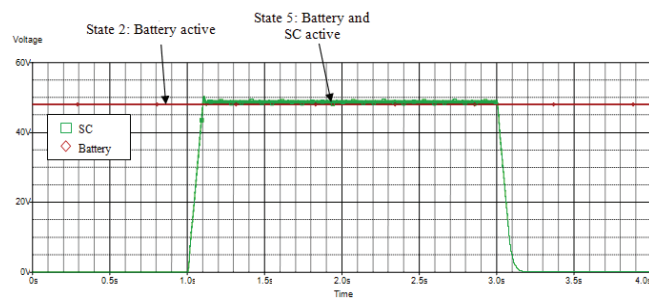At the state 5: $P_{load} = P_{battery} + P_{SC}$

Fig.15. Output systems in States 2 and 5

In Fig. 16, a simulation for the following terms is shown. The vehicle, for the first 3 s, is in State 2. Then, a high power demand is required that forces the system to activate the FC, which represents State 4. The EMS is still sensing the under power of the vehicle and makes decisions to trigger the SC. Subsequently, the system goes into State 7. When the simulation reaches 5 s, the battery capacity is critical and the system cuts off the battery supply, which is State 6. Then, the FC has to take over the entire power system, as the SC cannot longer supply energy, which is State 3. In this state, the battery and SC are recharged during low power demand and regenerative braking. The equation that can be related to the power load as:

At the state 6: $P_{load} = P_{FC} + P_{SC}$
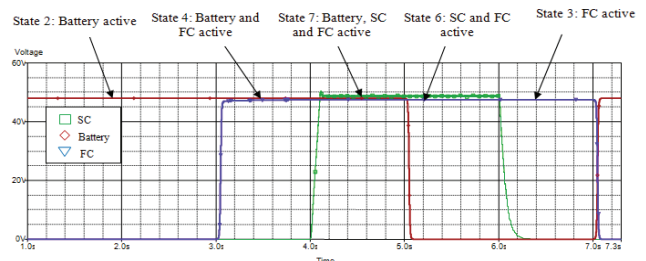At the state 7; $P_{load} = P_{battery} + P_{FC} + P_{SC}$

Fig. 16. Output systems at States 6 and 7

A sample of the supplied voltage (48 V) to the load is shown in Fig. 17 with a duty cycle of 0.5 and switching frequency of $f_r = 1$ kHz. This means only 50% of the supply voltage goes to the load. The drive frequency and x duty cycle can be varied depending on the demand load.
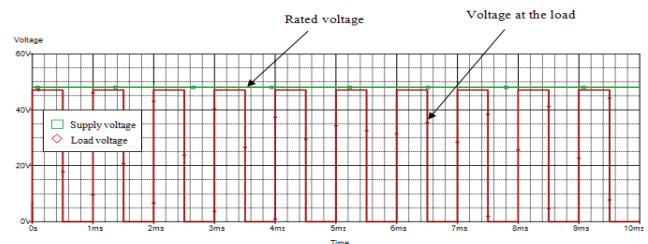

Fig.17. Motor drive signal to the load

The design circuit of the shunt regulator is shown in the previous figure and is used to charge the battery from the photovoltaic source. First, in the simulation design, the battery overcharge is set to be 48.4 V [22]. A reference voltage of 24 V is set on the positive input, and a voltage divider, R1 and R2, from the battery source is connected to the negative input voltages of the comparator. The output of comparator will turn ON the transistor depending on the difference between the input voltages. If the reference voltage is higher than voltage across R2, the shunt current at R3 equals zero (from Figure 18; 48.25pA), and excess power generated by the solar modules is not delivered to the battery. When the reference voltage is lower, the shunt current becomes negative (from Figure 19; –1.05A) and diverts current from the solar modules to charge the battery. Two different battery voltages are set at V6, which represents overcharge mode in Fig. 18 and charge mode in Fig. 19.
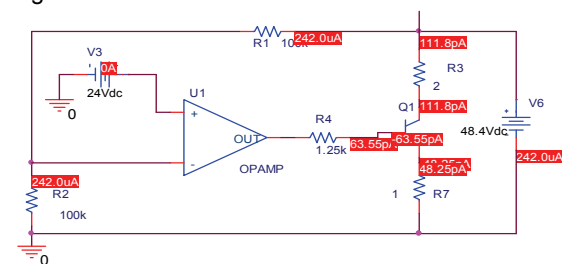

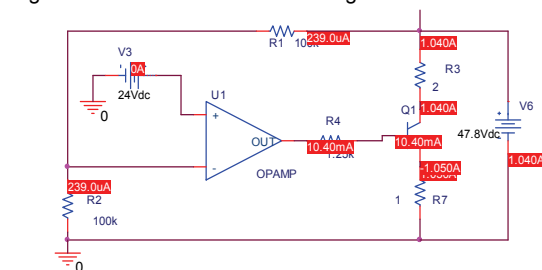Fig. 18. SHUNT current in overcharge mode

Fig. 19. SHUNT current in charge mode

Conclusion

The idea of using a PSPICE simulation is to model the general idea of an EMS and to evaluate a switching technique that maintains energy supply to the load. The input sensing sources, such as the battery SOC and speed detection for controlling system, are not yet designed in this system, which uses an open loop system. A closed loop control system will be studied and developed in the future with application for intelligent system, such as fuzzy logic or neural networks. Based on these PSPICE experiments, an FC hybrid vehicle has the potential to replace combustion engines if the EMS can coordinate all of the power sources perfectly. In this small power system, the battery plays a major role as the primary sources, as compared to other research work that assigns the battery as an auxiliary source. For this kind of power system, more research is required to measure the battery SOC and I-V characteristics so that a reliable and precise circuit design can be achieved. Furthermore, harvesting energy solar and plug-in accessories to charge the battery is another concept that may be realized in this system in the near future.

REFERENCES

[1] Mulhall P., Emadi A. Comprehensive Simulations and Comparative Analysis of the Electric Propulsion Motor for a Solar/Battery Electric Auto Rickshaw Three-Wheeler, *35th Annual Conference of IEEE on Industrial Electronics*, (2009), 3785-3750.
[2] Mullhall P., Lukic S. M., Wirasingha S. G., Young J. L., Emadi A. Solar-Assited Electric Auto Rickshaw Three-Wheeler, *IEEE Transaction on Vehicular Technology*,59(2010), 2298-2307.
[3] Gevorkian P. Sustainable Energy Systems Engineering, *McGraw Hill*, (2006).
[4] Mierlo J. V., den Bossche P. V.,l Maggeto G., Models of energy sources for EV and HEV: fuel cells, batteries, ultracapacitors, flywheels and engine-generators, Power Sources, 128(2004), 76-89.
[5] Garcia P., Fernandez L. M., Garcia C. A., Jurado F. Energy Management System of Fuel-Cell-Battery Hybrid Tramway, *IEEE on Industrial Electronics*, 57(2010), 4013-4023.
[6] Hannan M. A., Mohamed A. PSCAD/EMTDC Simulation of Unified Series-Shunt Compensator for Power Quality Improvement, *IEEE Transaction on Power Delivery*, 20(2005), 1650-1656.
[8] Beniak R. A formalised variable structure method of modelling converter drive, Przeglad Elektrotechniczny, 3(2009), 83-87.
[9] Merz H. Electric Machines and Drives, *VDE Verlag, Berlin*, (2002).
[10] Rashid M. H. Power Electronics circuits, Devices and Applications (Pearson Prentice Hall, New Jersey, 2004).
[11] Drabek T., Mikula S. Development of control system for the electric car, Przeglad Elektrotechniczny, 4(2011), 203-205.
[12] Fewson D. Introduction to Power Electronics (Arnold, London, 1998).
[13] Thounthong P., Chunkag V., Sethakul P., Sikkabut S., Pierfederici S., Davat B. Energy management of fuel cell/solar cell/supercapacitor hybrid power source, *Power Sources*, 128(2010), 313-324,.
[14] Ramani, K. Krishnan, A. New Hybrid Multilevel Inverter Fed Induction Motor Drive - A Diagnostic Study, *International Review of Electrical Engineering (IREE)*, 5(2010), No.6, 2562-2569.
[15] Thounthong P., Chunkag V., Sethakul P., Davat B., Hinaje M. Comparative Study of Fuel-Cell Vehicle Hybridization with Battery or Supercapacitor Storage Device, *IEEE Transaction on Vehicular Technology*, 58(2009), 3892-3904.
[16] Ahmed S., Chmielewski D. J. Load Characteristics and Control of a Hybrid Fuel Cell/Battery Vehicle, *American Control Conference*, (2009), 2654-2659.
[17] Azib T., Bethoux O., Marchand C., Berthelot E., Supercapacitors for Power Assistance in Hybrid Power Source with Fuel Cell, *35th Annual Conference of IEEE Industrial Elelctronics*, (2009), 3747-3752.
[18] Paplicki P. The new the generation of electrical machines applied in hybrid drive car, Przeglad Elektrotechniczny, 6(2010), 101-103.
[19] Basu S. Recent Trends in Fuel Cell Science and Technology, *Springer*,(2007).
[20] Ali T., Mohsen K. Adaptive passivity-based control of PEM fuel cell/battery hybrid power source, Przeglad Elektrotechniczny,4(2011), 164-171.
[21] Chao D. C-H., van Duijsen P. J., Hwang J. J., Liao C-H, Modelling of a Taiwan Fuel Cell Powered Scooter, *International Conference on Power Electronics and Drive System, PEDS* (2009), 913-919.
[22] Zenith F., Skogestad S. Control of fuel cell power output, *Journal of Process Control*, 17(2007), 333-347.
[22] Electric Double layer Capacitor, *Wikipedia*, (2010).
[23] Farcas C., Petreus D., Ciocan I., Palaghita N. Modeling and Simulation of Supercapacitors, *15th International Symposium for Design and Technology Packages, SIITME*, (2009), 195-200.
[24] Castaner L., Silvestre S. Modelling Photovoltaic Systems Using PSpice, *John Wiley & Sons, Inc.,* (2003).
[25] Lin B., Shen S. Analysis and Implementation of an Interleaved Buck Converter with High Power Factor, *International Review of Electrical Engineering (IREE)*, 5(2010), No.6, 2508-2515.
[26] Subiyanto., Mohamed A., Hannan M. A. Photovoltaic Maximum Power Point Tracking Controller Using a New High Performance Boost Converter, *International Review of Electrical Engineering (IREE),* 5(2010), No. 6, 2535-2545.
[27] Mecrow B.C., Bennet J.W., Jack A. G., Atkinson D. J., Freeman A. J. Drive Topologies for Solar-Powered Aircraft, *IEEE Transaction on Industrial Electronics*, 57(2010), 457-464.
[28] Maranda W., Piotrowicz M. Thermal modeling of photovoltaic modules under highly variable solar radiation, Przeglad Elektrotechniczny, 8(2010), 139
[29] Kendouci K., Mazari B., Behendria M. R. Speed Tracking Control of PMSM Using Backstepping Controller Simulation and Experimentation, *International Review of Electrical Engineering (IREE)*, 5(2010), No. 6, 2630-2636.
[30] Hannan M. A., Ghani Z. A., Mohamed A. An Enhanced Inverter Controller for PV Applications Using the dSPACE Platform, *in press International Journal of Photoenergy*, (2010).
[31] Ustun O., Yilmaz M., Gockce C., Karakaya U., Tuncay R. N. Energy Management Method for Solar Race Car Design and Application, *IEEE International on Electric Machines and Drives Conference,* (2009), 804-811.
[32] Zandi M., Payman A., Martin J. P., Pierfedereci S., Davat B., Tabar F. M. Energy Management of a Fuel Cell/Supercapacitor /Battery Power Source for Electric Vehicular Applications, *IEEE Transaction on Vehicular Technology,* 60(2011), 433-443,.
[33] Konatowski S., Dabrowski, M. Vehicle Positioning System, Przeglad Elektrotechniczny, 12(2008), 330-334.

Authors: *Associate Prof. Dr M A Hannan. Dept. of Electrical, Electronic & Systems Engineering, Universiti Kebangsaan Malaysia, 43600 Bangi, Selangor, Malaysia*
Corresponding author e-mail: hannan@eng.ukm.my